Journal of Renewable and Sustainable Energy

Life cycle assessment of hole transport free planar–mesoscopic perovskite solar cells

Cite as: J. Renewable Sustainable Energy **12**, 023502 (2020); https://doi.org/10.1063/1.5129784
Submitted: 02 October 2019 • Accepted: 19 February 2020 • Published Online: 10 March 2020

Huseyin Sarialtin, Roland Geyer and Ceylan Zafer

Journal of Renewable and Sustainable Energy ARTICLE scitation.org/journal/rse

Life cycle assessment of hole transport free planar–mesoscopic perovskite solar cells

Cite as: J. Renewable Sustainable Energy **12**, 023502 (2020); doi: 10.1063/1.5129784
Submitted: 2 October 2019 · Accepted: 19 February 2020 ·
Published Online: 10 March 2020

Huseyin Sarialtin,[1] Roland Geyer,[2] and Ceylan Zafer[3,a)]

AFFILIATIONS

[1]Department of Mechanical Engineering, Izmir Institute of Technology, Urla, 35430 Izmir, Turkey
[2]Bren School of Environmental Science and Management, University of California at Santa Barbara, Santa Barbara, California 93106, USA
[3]Solar Energy Institute, Ege University, Bornova, 35100 İzmir, Turkey

[a)]**Author to whom correspondence should be addressed:** ceylan.zafer@ege.edu.tr

ABSTRACT

Organo-metal lead halide perovskite solar cells (PSCs) attract attention due to their low cost and high power conversion efficiency. Some weak points of this technology are short lifetime, instability, and expensive metal electrode deposition. Eliminating the unstable hole transport layer (HTL) and using carbon-based materials as the counter electrode would address both. In this work, we present a cradle-to-gate life cycle assessment of two HTL-free PSC designs, which use solution phase deposition to achieve mesoscopic and planar structures. Environmental impacts of producing 1 m^2 PSCs are converted to impacts per kWh electricity generation assuming 5 years of operational lifetime. We find that major impacts come from fluorine doped tin oxide (FTO) glass patterning due to the electricity consumption of FTO patterning and glass cleaning processes. Even though the electricity consumption when manufacturing both PSCs is similar, their different efficiencies make the environmental impacts per kWh of electricity higher for the mesoscopic PSC than for the planar PSC. Energy payback time values of planar PSCs and mesoscopic PSCs are 0.58 and 0.74 years, respectively, and these values are shorter than those of commercial first and second generation solar cells. However, the global warming potential (GWP) values of planar and mesoscopic PSCs are 75 and 94 g CO_2-eq/kWh, respectively, and these values are still higher than those of commercial solar cells. To reach the GWP of commercial cells, the operational lifetime would have to be 8 and 10 years for planar and mesoscopic PSCs, respectively.

I. INTRODUCTION

Global energy production continues to grow and still relies predominantly on fossil fuels. A major shift to renewable energy sources is increasingly seen as the most important strategy to mitigate the anthropogenic climate change and other environmental impacts caused by fossil fuel use. Photovoltaics is one of the most promising renewable energy technologies and converts essentially unlimited solar energy into electrical energy with significantly lower environmental impacts than any fossil source. The continuous decrease in the cost of photovoltaic technologies has led to a dramatic increase in investment and installation in recent years. Today's installed photovoltaic capacity of 480 GW is expected to reach 2840 GW by 2030.[1] Currently installed photovoltaic capacity largely consists of (mono- and polycrystalline) silicon solar cells. In addition, thin film technologies (CdTe and Copper Indium (Gallium) Sulfide (CIGS)), also known as second generation technology, are gaining market share due to low manufacturing cost. Even more recently, researchers have focused to develop new photovoltaic architectures by using organic semiconductors to produce even more cost-effective devices. Organic and dye sensitized solar cells are some examples of this third generation of solar cells produced by solution-based fabrication techniques. One especially promising third generation technology is organic-inorganic perovskite solar cells (PSCs), which have become very popular in recent years.[2]

Perovskite is a general name given to compounds with the same crystal structure as $CaTiO_3$, which was discovered by Russian material scientist Lev Perovsky.[3] This crystal structure can be expressed as ABX_3. In this octahedron cube structure, large cations are expressed by A and small cations in the center by B, and X stands for halogens. With the diversity of cations in parts A and B, this crystal structure becomes a compound with different properties such as optical and charge transport.[4] Perovskite materials used in solar cells are organo-metallic (hybrid) perovskites.[5] Organo-metal lead halide perovskite was first used as an active light harvesting layer in a photovoltaic cell with an efficiency of 3.8% in 2009.[6] With solid electrolyte usage, the

power conversion efficiency of perovskite solar cells increased to about 10% in 2012.[7] Since then, the cell efficiency has progressed rapidly and achieved 25.2% today.[8] The operational lifetime (LT) is still a problem of this technology. Currently, there is not sufficient outdoor stability of PSCs.[9]

Even though photovoltaic cells are low-carbon energy sources, some greenhouse gas emissions occur during cell production and all upstream processes. Determining the environmental performance of a photovoltaic cell therefore requires life cycle assessment (LCA). Using this method, the energy payback time (EPBT), greenhouse gas emissions, and other environmental impacts can be quantified.[10] A large number of studies have been published, which examine the environmental performance of first and second generation solar cells. Since perovskite solar cells are still a very new technology, environmental assessments are still sparse and uncertain. Prior to the commercialization of perovskite solar cells, it is important to examine their environmental impacts, such as carbon emissions, acidification, or ecotoxicity, to prevent unintended consequences. Due to the stability problem of Spiro-OMETAD, which is the most preferred hole transport layer (HTL), and the expensive production of metal back electrodes, HTL-free devices recently have been the focus of researchers.[11] In these devices, the hole transport layer is eliminated, and carbon-based electrode materials are used for both hole transport and the back electrode. Although elimination of the hole transport layer results in a loss of efficiency in the cell, recent work has shown that the HTL-free architecture has achieved a power conversion efficiency of 16%.[12] Moreover, it has been shown that this cell architecture costs half as much as the classical architecture.[13] Generally, HTL-free perovskite cell devices are based on mesoscopic cell structures. However, a recent study has shown that the efficiency of planar HTL-free cells (11.5%–14.5%) can be higher than that of mesoscopic HTL-free devices (7%–12.5%).[14]

In this paper, we therefore perform life cycle assessments of two HTL-free architectures, one planar and one mesoscopic, as described in the original publication.[14] As the article we refer suggests, solution-based spin-coating fabrication was the preferred method for manufacturing perovskite and electron transport layers (ETLs). Besides, the doctor blading fabrication method was chosen to produce the back electrode. We noticed that much of the previous LCA work on perovskite solar cells compares architectures that contain different variations. However, the wide variation makes insightful comparisons between devices difficult. We therefore study two devices that are only different in the planar and mesoscopic architectures of their ETLs. This allows us to determine the environmental performance of two variants of HTL-free devices and compare these planar and mesoscopic devices with commercial photovoltaic (PV) technologies and some previous LCA work on PSCs.

II. DEVICE ARCHITECTURES

The two representative HTL-free devices we analyze have shown great performance in a recent article.[14] As seen in Fig. 1, both architectures have the carbon back electrode, fluorine doped tin oxide (FTO) coated glass, and perovskite layers in common. However, the planar device has SnO_2 as the electron transport layer, while the mesoscopic device has TiO_2. The mesoscopic device has an additional thin TiO_2 blocking layer (BL) in its architecture. In the reference work, the thickness of perovskite and carbon electrode layers was given as 500 nm and 20 μm, respectively. Thicknesses of other layers are assumed based on the literature. In typical mesoscopic PSC architecture, the mesoporous TiO_2 thickness varies between 160 and 480 nm and the compact TiO_2 thickness varies between 35 and 80 nm.[15] Therefore, we selected 300 nm thickness for the mesoporous TiO_2 layer and 60 nm thickness for the compact blocking TiO_2 layer. In the planar device, the thickness of SnO_2 is selected as 100 nm, which is an average literature value for this layer.[16] FTO coated glass is assumed as 0.7 mm glass and the front electrode layer thickness as 180 nm, based on the work of García-Valverde *et al.*[17]

In the reference work, the power conversion efficiency of planar PSCs varies between 11.5% and 14.5% and that of mesoscopic PSCs between 7% and 12.5%. We selected the highest efficiency value (14.5%) for the planar PSC device by the benefit of the literature.[18] Recent work showed that power conversion efficiencies of mesoscopic PSC devices that use TiO_2 as an electron transport layer are around 8% and 12%.[13] So, we selected 11.5% for the mesoscopic PSC.

FTO coated glass is patterned and cleaned with ethanol and acetone in an ultra-sonication process. Then, the ETL layer is deposited using the spin-coating technique. In this work, the conventional solution-based spin coating fabrication technique is assumed for the manufacture of all layers except the carbon back electrode, for which deposition by blade coating is assumed. A 2×2 in.^{2} cell area is chosen in spin coating fabrication, and all spin-coating processes are applied for 30 s. In the planar device, after deposition of the SnO_2 ETL layer, a 180 °C annealing process is applied for 1 h. In the mesoscopic device, after deposition of the blocking TiO_2 layer and the mesoporous TiO_2 layer, a 450 °C annealing process is applied for 30 min each. For the fabrication of the perovskite layer, a two-step spin coating process is modeled. Methylammonium iodide (CH_3NH_3I) and lead iodide (PbI_2) are applied separately on a substrate. After deposition of the layer, a 100 °C annealing process is applied. At last, carbon black is coated by the doctor blade technique.

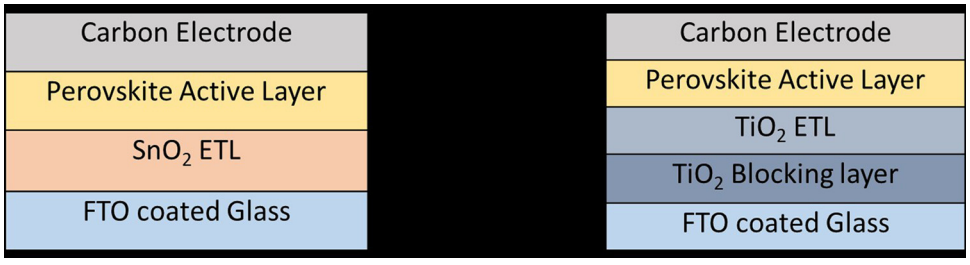

FIG. 1. Perovskite solar cell architectures, following planar HTL-free (left) and mesoscopic HTL-free (right) as reported in Ref. 14.

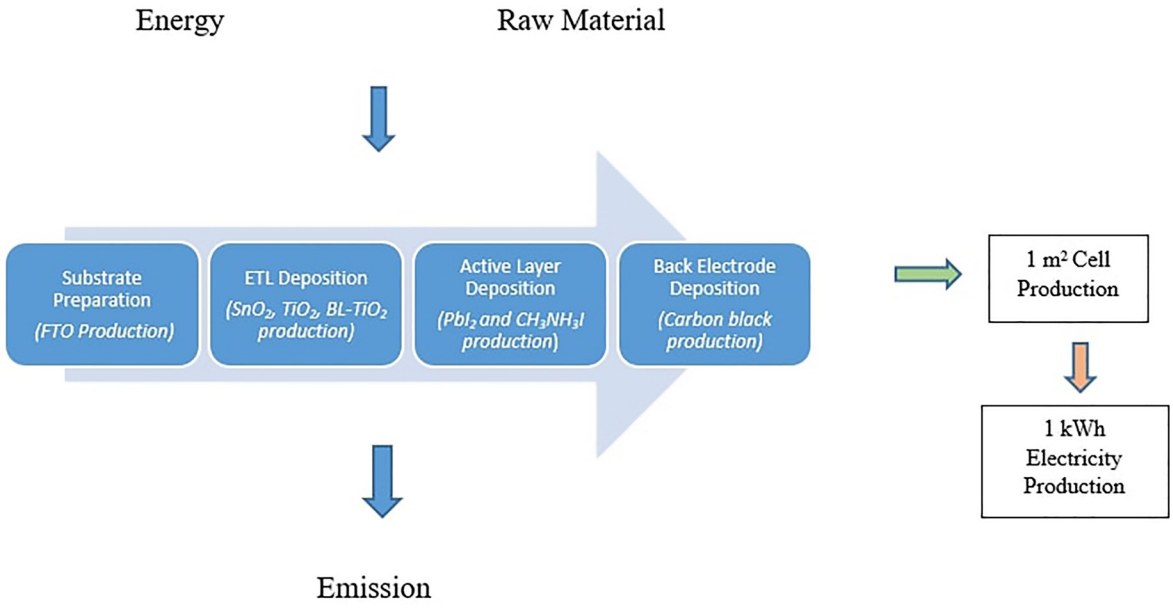

FIG. 2. System boundary considered in the LCA study for perovskite solar cell devices.

III. METHODOLOGY

A. Goal and scope

LCAs assess the environmental impacts of a product through its life cycle from raw material supply to the end of life or parts thereof. The aim of this study is to quantify the potential environmental impacts of two HTL-free perovskite solar cells. The initial functional unit chosen for this assessment is the manufacturing of 1 m^2 cells. A secondary functional unit is 1 kWh of electricity production. Initially, inventory data for the production of 1 m^2 solar cells have been collected and converted to potential environmental impacts. In a second step, the environmental impact results for both devices are converted to impact indicators for 1 kWh electricity production (see the following equation):

$$Impact_{\mathrm{kWh}} = \frac{Impact_{\mathrm{m^2}}}{I \times \eta \times A \times PR \times LT}. \quad (1)$$

Here, I is the insolation constant (kWh/m^2 yr), η is the module efficiency (%), A is the active cell area (m^2), PR is the performance ratio (%), LT is the lifetime of the cell (yr), $Impact_{\mathrm{m^2}}$ is the impact per 1 m^2 cell area, and $Impact_{\mathrm{kWh}}$ is the impact per 1 kWh electricity generation.

The system boundary for this LCA is cradle to gate, i.e., from raw material supply and manufacturing processes to the finished solar cell (Fig. 2).

To calculate the energy payback time (EPBT), solar insolation is chosen as 1700 kWh m^2 yr, which represents southern Europe.[19] Recent work has shown that perovskite solar cells need to have at least a 5-year lifetime in order to compete with commercial solar cells in terms of CO_2 emissions.[20] Therefore, the lifetime of both PSC devices is assumed to be 5 years. Two important factors that affect cell electricity output are its performance ratio and active area. The performance ratio is described as the ratio between actual and theoretical energy output.[21] The active area is defined as the percentage of the actively working cell area. We assumed the performance ratio as 80% and the active area as 75%. These are typical values used in previous LCA studies.[22,23] The efficiency of a solar cell is commonly determined in a small cell area. A module consists of several cells, and its efficiency is lower than the measured efficiency of individual solar cells. Previous research shows that cell-to-module efficiency losses vary between 20% and 50% in commercial PVs.[24] In this study, we have selected a loss value of 20% for PSCs. All parameter specifications are shown in Table I.

EPBT is defined as the amount of time required by a PV technology to offset the primary energy demand of producing it. This paper only assesses solar cell production, excluding all downstream processes such as the balance of system production, PV system assembly, operation, and maintenance. Therefore, EPBT is calculated based on the cradle-to-gate primary energy demand for cell production only [see Eq. (2)].[25] The factor $\varepsilon = 0.35$ converts the cell's electricity output into primary energy demand,

$$EBPT = \frac{Primary\ energy\ demand}{(I \times \eta \times A \times PR)/\varepsilon}. \quad (2)$$

TABLE I. Specifications of planar and mesoscopic PSC devices.

Active area	75%
Performance ratio	80%
Cell to module efficiency loss	20%
Annual solar insolation	1700 kWh m^2 yr
Planar PSC efficiency	14.50%
Mesoscopic PSC cell efficiency	11.50%

B. Life cycle inventory

Life cycle inventory (LCI) analysis includes the estimation of electricity consumption and material usage during solar cell manufacturing and the required upstream and downstream processes. In this work, literature data and Ecoinvent v3.4 have been used to create the inventory tables that can be found in the supplementary material. We have made adaptations (laboratory synthesis) for some chemical compounds that are not available in databases with the help of the literature.

Energy consumption data for FTO glass patterning, spin coating, doctor blade coating, and annealing processes were also taken from

TABLE II. Inventory table of manufacturing both planar and mesoscopic HTL-free perovskite solar cells. I stands for material input and P for the process energy requirement. All emission values and chemical synthesis are showed in detail in the supplementary material. The * indicates detailed inventory data of TiO_2 production presented in the supplementary information document.

Input materials		Amount	Unit	Comments	References
FTO front electrode					
I	Fluorine, liquid, at plant	6.74×10^{-6}	kg		27
I	Oxygen, liquid, at plant	9.1×10^{-3}	kg		27
I	Tin, at regional storage	2.19×10^{-4}	kg		27
I	Flat glass, uncoated, at plant	1.54	kg		27
I	Acetone, liquid, at plant	1.60×10^{-2}	kg		17,28
I	Ethanol from ethylene, at plant	1.60×10^{-2}	kg		17,29
P	US: electricity, production mix US (FTO, patterning, and ultra-sonication)	106.43	MJ		23,27
TiO_2 BL layer				Assumed 60 nm BL layer thickness Density = 4.23 g/cm^3	
	TiO_2 production*	5.08×10^{-3}	kg		30,31
P	US: electricity, production mix US [spin coating and annealing (450 °C, 30 min)]	23.61	MJ		17,23
TiO_2 ETL layer				The thickness of the TiO_2 ETL layer is assumed to be 300 nm 18 wt. % TiO_2 in methyl methacrylate (MMA)	
I	TiO_2 production*	1.28×10^{-3}	kg		15,32
I	Methyl methacrylate (MMA)	5.4×10^{-3}	kg		
P	US: electricity, production mix US [spin coating and annealing (450 °C, 30 min)]	23.61	MJ		23,27
SnO_2 ETL layer				The thickness of SnO_2 is assumed as 100 nm The density of SnO_2 is 6.95 g/cm^3	
	SnO_2 production	13.9×10^{-3}	kg		16
P	US: electricity, production mix US [spin coating and annealing (450 °C, 30 min)]	46.33	MJ		17,23
Perovskite active layer				The thickness of the active layer is 500 nm The density of methyl ammonium lead iodide is 1.368 g/ml	14,33
I	PbI_2 production	1.02×10^{-2}	kg		
I	N,N-dimethylformamide, at plant	14.2×10^{-3}	kg	Density of Dimethylformamide (DMF) = 0.95 g/ml	34
I	CH_3NH_3I production	3.51×10^{-3}			
P	US: electricity, production mix US [spin coating and annealing (100 °C, 1 h)]	47.23	MJ		17,23
Back electrode					
I	Carbon black production	0.4	kg	Density of amorphous carbon assumed as 2.1 g/cm^3	35
P	US: electricity, production mix US (doctor blading coating)	3.6	MJ		36

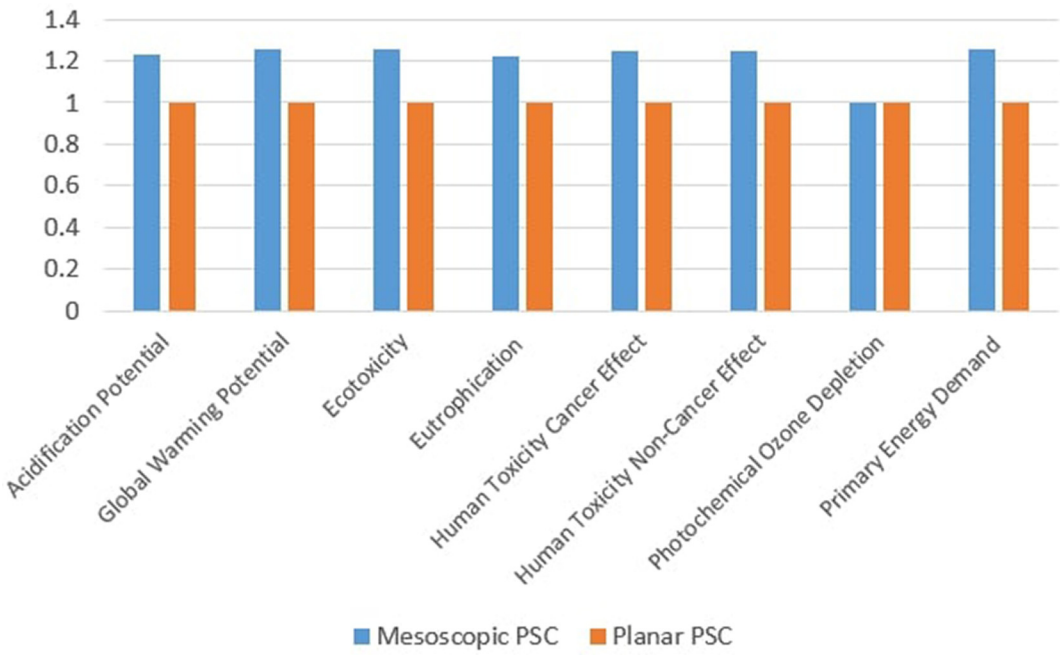

FIG. 3. Comparison environmental impacts by taking the values of planar PSCs as unit.

the literature. Compounds that are necessary for production, which are not available in the Ecoinvent database, are synthesized as described in the literature assuming 100% reaction efficiency. Energy requirements for the chemical syntheses are omitted because they are small in comparison with other energy requirements.[17]

Material yields during manufacturing are extremely low. The literature suggests material loss in the spin coating process as 95%.[26] After determining the material content of the ETL or perovskite layers, we use the material loss estimate to calculate the total material input. Volatile compounds from thermal annealing and chemical reactions were modeled as emission to air. Materials that are lost during spin coating were modeled as waste materials.

Summaries of the life cycle inventories for both HTL-free PSCs are shown in Table II. Chemical synthesis reaction inputs and emissions are presented in a complementary inventory table in the supplementary material (Table S1).

C. Life cycle impact assessment

Eight midpoint environmental impact categories were used for impact assessment using the International Refference Life Cycle Data System (ILCD) impact assessment models. They are acidification (Mole of H+ eq.), climate change (kg CO_2 eq.), ecotoxicity (CTUe), eutrophication (kg N eq.), human toxicity cancer effects (CTUh), human toxicity non-cancer effects (CTUh), photochemical ozone formation (kg NMVOC eq.), and primary energy demand (MJ). The eight ILCD impact categories chosen were mostly used in previous LCA works. The photochemical ozone depletion impact category is first studied in our research besides previous reports. Contribution analysis is used to show the relative environmental significance of each layer for each impact category. To enable comparability across PV technologies, we have converted global warming potential (GWP) results from 1 m^2 cell production to 1 kWh electricity generation. All results were calculated with characterization factors provided by Gabi 8.1 software with Gabi and Ecoinvent databases.

IV. RESULTS AND DISCUSSION

In Fig. 3, we show environmental impact scores per 1 kWh electricity production of both PSCs. Mesoscopic and planar impact values are compared based on the values of planar PSCs as unit. Accordingly, the mesoscopic PSC has 1.2 times higher impact values than the planar

TABLE III. Total environmental impact values of PSC architectures for 1 kWh electricity production.

Environmental impact categories	Planar PSC	Mesoscopic PSC
Acidification potential (mole of H+ eq.)	6.49×10^{-4}	7.99×10^{-4}
Global warming potential (kg CO_2 eq.)	0.075	0.094
Ecotoxicity (CTUe)	0.353	0.443
Eutrophication (kg N eq.)	6.94×10^{-4}	8.50×10^{-4}
Human toxicity cancer effect (CTUh)	4.15×10^{-9}	5.16×10^{-9}
Human toxicity non-cancer effect (CTUh)	1.42×10^{-8}	1.77×10^{-8}
Photochemical ozone depletion (kg NMVOC eq.)	2.50×10^{-4}	2.49×10^{-4}
Primary energy demand (MJ)	1.257	1.579

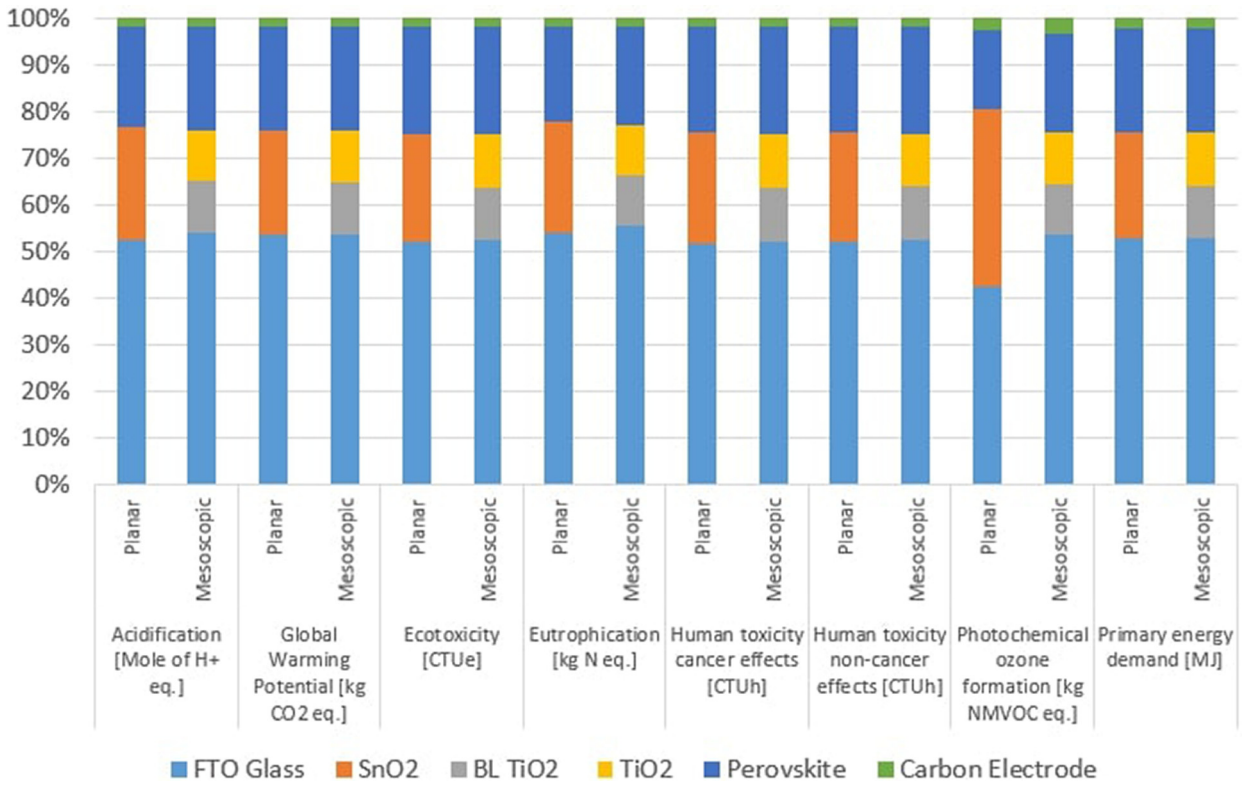

FIG. 4. Environmental impact score share of both PSCs by the layer.

PSC in seven categories. Photochemical ozone depletion is the only environmental impact category that the values of both PSCs are almost equal.

Since the different types of environmental impacts are calculated in different units, they are not directly comparable to each other. To clarify Fig. 3, we provide exact impact values in Table III.

As can be seen in Fig. 4, more than half of the impact scores stem from FTO glass. ETL and perovskite layers show similar contributions, while the share of the carbon electrode is just around 2%. Environmental impact score shares of both PSCs show similar results because of their similar manufacturing electricity consumption. Only in the photochemical ozone formation impact category, the SnO_2 ETL layer impact share is almost twice as high as the sum of ETL and blocking layer in the mesoscopic PSC.

In Table IV, we list electricity impact contribution of both devices by ILCD impact categories. Electricity consumption is responsible for more than 90% impact values in almost all categories.

A. Manufacturing electricity demand and energy payback time

The electricity demand for the manufacturing of each layer of the PSCs is shown in Fig. 5. Added together, the manufacturing electricity consumption is 203 MJ for the manufacturing of 1 m^2 planar PSCs and 204 MJ for mesoscopic PSC manufacturing. The manufacturing electricity demands for both devices are thus very similar. This is because the annealing duration of the ETL layer in the planar device is equal to the sum of the two TiO_2 layers in the mesoscopic device. The small difference is due to the use of one more spin coating process in the mesoscopic architecture. Since the planar architecture does not use a blocking layer, no additional spin coating process is required.

The largest fraction of the electricity consumption of manufacturing PSC devices is due to the annealing processes (44%). Annealing was used for the production of all layers except FTO glass and carbon counter electrode.

The highest manufacturing electricity demand share (106.23 MJ/m^2, 52%) is in the FTO-glass patterning in both devices (Fig. 4). In previous LCA studies, Espinosa *et al.*[27] did not evaluated the cleaning process for FTO-glass patterning and Celik *et al.*[23] did not evaluated

TABLE IV. Contribution (%) of electricity consumption on the environmental impacts of both PSCs.

Environmental impact category	Planar PSC	Mesoscopic PSC
Acidification potential	97	93
Global warming potential	95	94
Ecotoxicity	98	97
Eutrophication	92	89
Human toxicity cancer effect	98	98
Human toxicity non-cancer effect	98	97
Photochemical ozone depletion	92	72

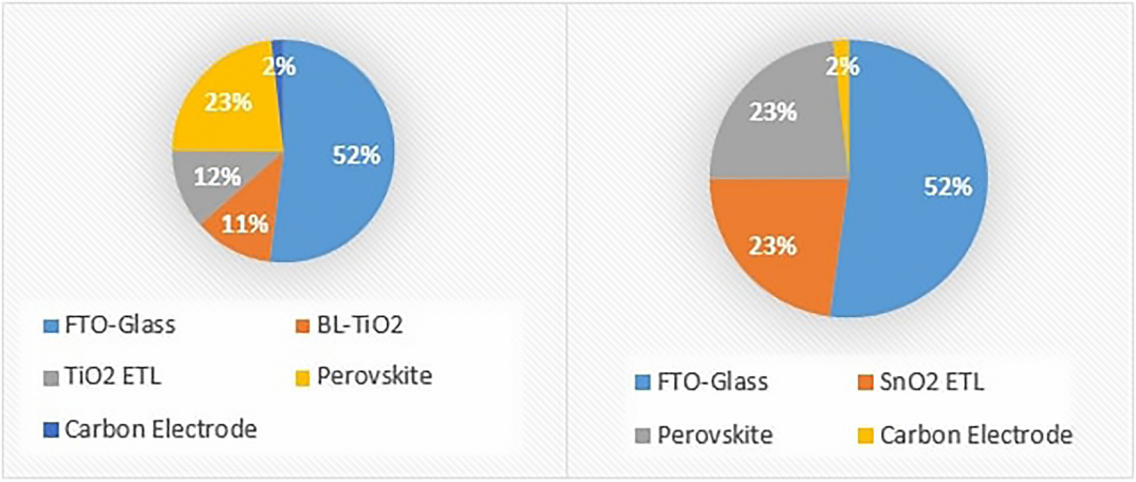

FIG. 5. Manufacturing electricity demand of each layer of both HTL-free PSCs (MJ/m^2), manufacturing electricity demand percentages of each layer of mesoscopic PSCs (left) (total 204 MJ), and manufacturing electricity demand percentages of each layer of planar PSCs (right) (total 203 MJ).

the electricity requirement to deposition of FTO on a glass substrate. Therefore, the manufacturing electricity values for FTO patterning are lower in these works (36 and 70 MJ, respectively). In this study, the amount of manufacturing electricity exceeded 100 MJ due to the involvement of both processes in the account.

In this work, we determined primary energy demands as 741 MJ for mesoscopic PSCs and 744 MJ for planar PSCs. We compared our EPBT results of planar and mesoscopic devices with commercial mono and poly silicon PVs and thin film Cdte PVs. As can be seen in Fig. 6, both PSC devices of our study have better EPBT results than commercial PVs[37] and PSC designs from previous studies.[23,27]

B. Global warming potential

Global warming potential values of commercial PVs vary between 29 and 50 g CO_2-eq per kWh electricity production.[37] According to our Life Cycle Impact Assessmen LCIA results, we have found that GWP values of planar and mesoscopic PSCs are 75 and

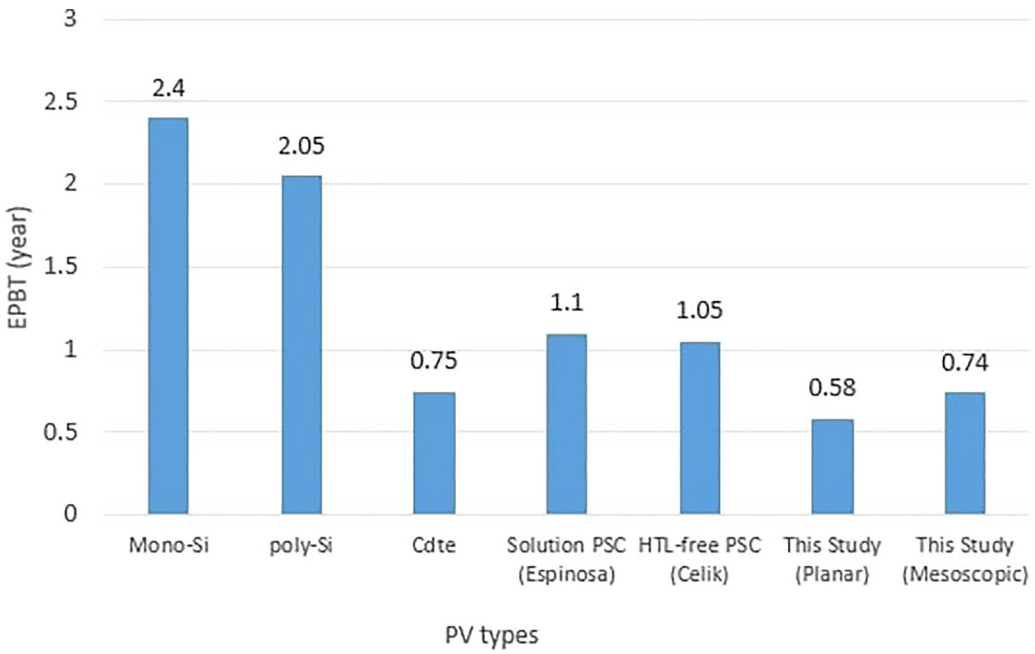

FIG. 6. Energy payback time comparison of planar and mesoscopic HTL-free PSCs with commercial PVs and previous LCA studies.

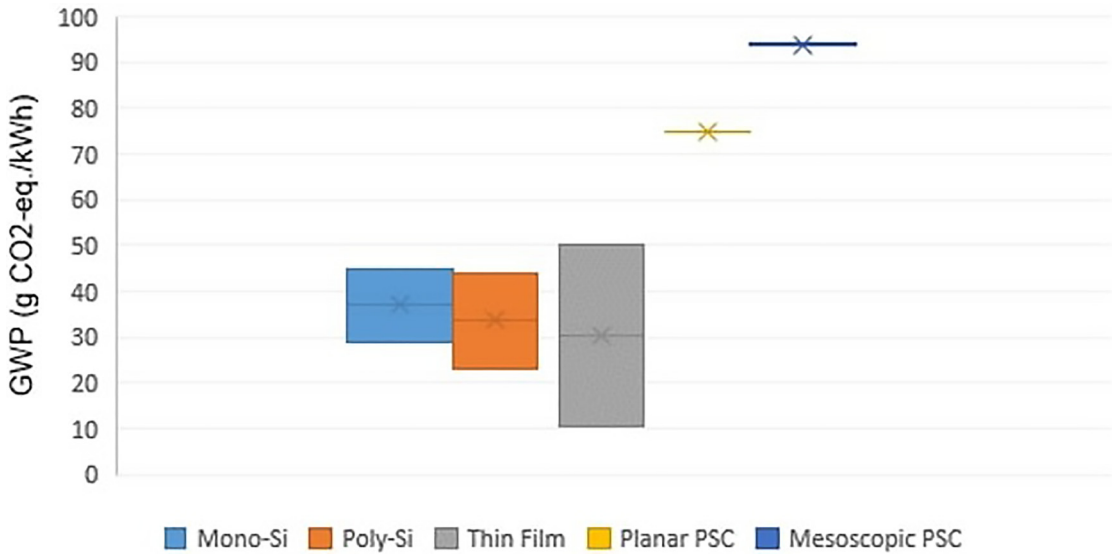

FIG. 7. Comparison of planar and mesoscopic PSCs in this study with commercial PV technologies[37] in terms of GWP results.

94 g CO_2-eq/kWh, respectively. As can be seen in Fig. 7, both PSCs have higher GWP values than commercial PVs. Previous LCA works report a GWP value of 350 g CO_2-eq for a conventional solution-based perovskite solar cell[27] and 99 g CO_2-eq for a hole-transport-free perovskite cell.[23] Therefore, our results are lower than previous PSC LCA work but still higher than commercial PV technologies.

We also investigated how much of the GWP comes from electricity consumption and raw material usage. We found that in the planar device, 95% of GWP impact is from electricity consumption. The fraction is 96% for the mesoscopic device. We also examined the contribution of each material in detail. As seen in Fig. 8, in the planar device, most of the raw material impact comes from flat glass (73%), followed by tin (16%), carbon black (5%), and all others (6%). In the mesoscopic device, 85% of raw material impact is from flat glass, 5% from carbon black, and 10% from all others. So, as far as the ETL layer is concerned, it can be seen that tin has a higher GWP contribution than the titanium dioxide. In previous work, it was shown that tin-based perovskite devices have a higher environmental impact than the lead based perovskite solar cells. This work corroborates that tin usage in perovskite solar cells causes a significant GWP impact.

We also conducted a sensitivity analysis to determine how much lifetime is required to achieve a competitive GWP value relative to commercial PVs. As shown in Fig. 9, GWP values decline with the increasing lifetime of the devices. If we consider that the highest GWP

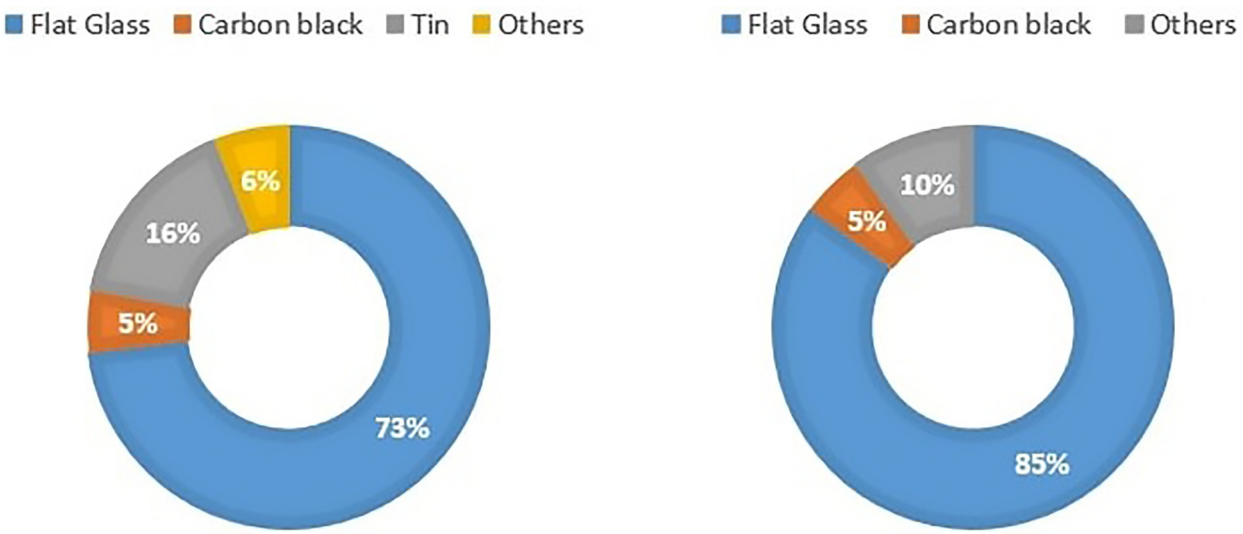

FIG. 8. Effect of raw material extraction on the GWP value for both planar (left) and mesoscopic (right) PSC devices.

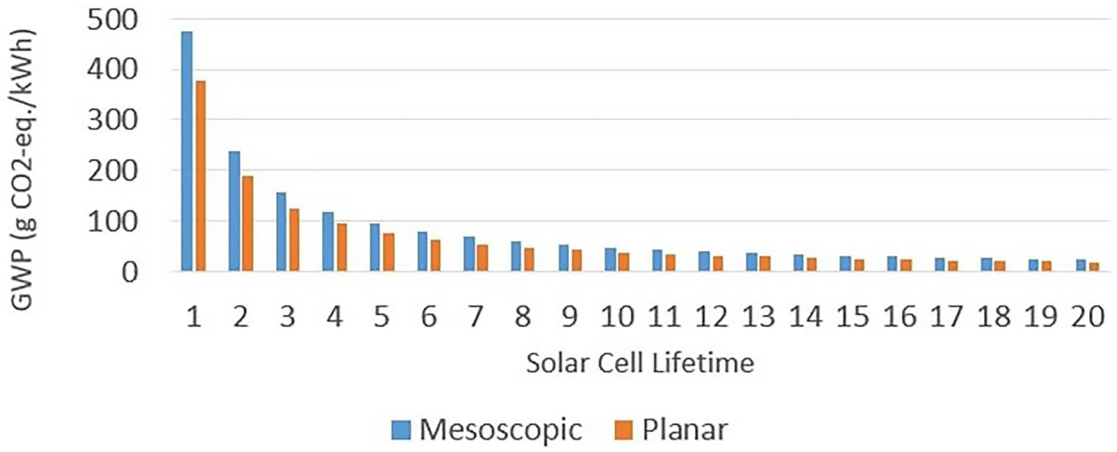

FIG. 9. Sensitivity analysis of GWP values of mesoscopic and planar PSCs.

value of commercial PVs is around 50 g CO_2-eq, planar PSCs need 8 years and mesoscopic PSCs need 10 years to achieve an equal value. Manufacturing 1 m^2 planar and mesoscopic PSCs has almost identical GWP. However, planar PSCs with per kWh of electricity output have lower GWP than mesoscopic PSCs. This is because the planar device has higher conversion efficiency and thus needs less cell area than the mesoscopic PSC to generate 1 kWh electricity.

V. CONCLUSION AND FUTURE WORK

Our environmental assessment of manufacturing hole transport free perovskite solar cells shows that the majority of environmental impacts comes from electricity consumption in all environmental impact categories. Following FTO glass patterning, annealing processes, which are used during the production of the blocking layer, ETL, and perovskite active layer, are major contributors to total electricity consumption. In contrast to previous LCA works, FTO-coated glass contributes the most to the cradle-to-gate impacts of the PSCs studied in our work (52%). We determined that there were some missing assumptions about cleaning and FTO production in previous works.

We present lower EPBT results by using low electricity consumptive spin coating and blade coating fabrication techniques for deposition of perovskite and carbon black electrode layers compared to data presented by Celik *et al.* wherein the spray coating technique was selected.

Per kWh, the GWP impact of mesoscopic PSCs is higher than that of planar PSCs. However, both impact scores are higher than those for commercial PVs. We determined that 95%–96% of GWP impacts stem from electricity consumption. In both devices, the impact from raw material extraction is small and mostly comes from FTO-coated glass. Compared to other materials, Sn stands out as having relatively high impact scores. We applied a sensitivity analysis and showed that planar devices need at least 8 years and mesoscopic devices at least 10 years to achieve a GWP value below 50 g CO_2 per kWh, which is the high end of what is reported for commercial PVs.

Because of the short operational lifetime of the PSCs, lifetime electricity production is low when compared to commercial PVs. Despite the good conversion efficiencies of today's PSCs, their production impacts are still divided over a relatively small lifetime electricity output. This makes the environmental impacts per kWh still too high to be competitive with those of commercial PVs. Our LCA demonstrates that the elimination of the hole transport layer in solution-based perovskite solar cells reduces the manufacturing energy demand and thus energy payback time. Nevertheless, increasing the operational lifetime of PSCs is still a priority in order to reduce their global warming potential to the level of commercial PVs. Besides, since spin coating is not suitable for large-scale applications, it will be useful to examine methods suitable for serial production such as slot die in the future.

SUPPLEMENTARY MATERIAL

See the supplementary material for the all emission values and chemical synthesis in detail.

ACKNOWLEDGMENTS

This work was supported by the Scientific and Technological Research Council of Turkey (No. TUBITAK BIDEB 2214/A).

REFERENCES

[1]International Renewable Energy Agency, *Future of Solar Photovoltaic* (International Renewable Energy Agency, 2019).
[2]L. Qiu, L. K. Ono, and Y. Qi, Mater. Today Energy **7**, 169–189 (2018).
[3]L. J. Schmidt, in 38th Rochester Mineral Symposium Program Notes (2011), pp. 31–32.
[4]Z. Song, S. C. Watthage, A. B. Phillips, and M. J. Heben, J. Photonics Energy **6**, 022001 (2016).
[5]L. K. Ono, N.-G. Park, K. Zhu, W. Huang, and Y. Qi, ACS Energy Lett. **2**, 1749–1751 (2017).
[6]A. Kojima, K. Teshima, Y. Shirai, and T. Miyasaka, J. Am. Chem. Soc. **131**, 6050–6051 (2009).
[7]H. S. Kim, C. R. Lee, J. H. Im, K. B. Lee, T. Moehl, A. Marchioro, S. J. Moon, R. Humphry-Baker, J. H. Yum, J. E. Moser, M. Grätzel, and N. G. Park, Sci. Rep. **2**, 591 (2012).
[8]See https://www.nrel.gov/pv/cell-efficiency.html for "Best Research-Cell Efficiency Chart, Photovoltaic Research, NREL" (last accessed December 28, 2019).
[9]A. Mei, X. Li, L. Liu, Z. Ku, T. Liu, Y. Rong, M. Xu, M. Hu, J. Chen, Y. Yang, M. Grätzel, and H. Han, Science **345**, 295–298 (2014).

[10]J.-A. Alberola-Borràs, R. Vidal, and I. Mora-Seró, Sustainable Energy Fuels **2**, 1600–1609 (2018).
[11]Y. Yang, J. Xiao, H. Wei, L. Zhu, D. Li, Y. Luo, H. Wu, and Q. Meng, RSC Adv. **4**, 52825–52830 (2014).
[12]H. Zhang, H. Wang, S. T. Williams, D. Xiong, W. Zhang, C. C. Chueh, W. Chen, and A. K. Y. Jen, Adv. Mater. **29**, 1606608 (2017).
[13]S. Maniarasu, T. B. Korukonda, V. Manjunath, E. Ramasamy, M. Ramesh, and G. Veerappan, Renewable Sustainable Energy Rev. **82**, 845–857 (2018).
[14]S. Lin, B. Yang, X. Qiu, J. Yan, J. Shi, Y. Yuan, W. Tan, X. Liu, H. Huang, Y. Gao, and C. Zhou, Org. Electron. **53**, 235–241 (2018).
[15]J. Li, J. X. Yao, X. Y. Liao, R. L. Yu, H. R. Xia, W. T. Sun, and L. M. Peng, RSC Adv. **7**, 20732–20737 (2017).
[16]J. Duan, Q. Xiong, B. Feng, Y. Xu, J. Zhang, and H. Wang, Appl. Surf. Sci. **391**, 677–683 (2017).
[17]R. García-Valverde, J. A. Cherni, and A. Urbina, Prog. Photovoltaics: Res. Appl. **18**, 535–538 (2010).
[18]L. Xiong, Y. Guo, J. Wen, H. Liu, G. Yang, P. Qin, and G. Fang, Adv. Funct. Mater. **28**, 1802757 (2018).
[19]See http://globalsolaratlas.info/ for "Global Solar Atlas" (last accessed June 29, 2018).
[20]T. Ibn-Mohammed, S. C. L. Koh, I. M. Reaney, A. Acquaye, G. Schileo, K. B. Mustapha, and R. Greenough, Renewable Sustainable Energy Rev. **80**, 1321–1344 (2017).
[21]T. Dierauf, A. Growitz, S. Kurtz, J. L. B. Cruz, E. Riley, and C. Hansen, "Weather-corrected performance ratio," Report No. NREL/TP-5200-57991 (2013).
[22]J. Gong, S. B. Darling, and F. You, Energy Environ. Sci. **8**, 1953–1968 (2015).
[23]I. Celik, Z. Song, A. J. Cimaroli, Y. Yan, M. J. Heben, and D. Apul, Sol. Energy Mater. Sol. Cells **156**, 157–169 (2016).
[24]S. B. Darling and F. You, RSC Adv. **3**, 17633–17648 (2013).
[25]K. P. Bhandari, J. M. Collier, R. J. Ellingson, and D. S. Apul, Renewable Sustainable Energy Rev. **47**, 133–141 (2015).
[26]N. Sahu, B. Parija, and S. Panigrahi, Indian J. Phys. **83**, 493–502 (2009).
[27]N. Espinosa, L. Serrano-Luján, A. Urbina, and F. C. Krebs, Sol. Energy Mater. Sol. Cells **137**, 303–310 (2015).
[28]See https://www.aqua-calc.com/page/density-table/substance/acetone for "Aqua-Calc" (last accessed June 25, 2018).
[29]See https://www.sigmaaldrich.com/catalog/product/sigald/24102?lang=en&region=US for "Sigma-Aldrich" (last accessed June 25, 2018).
[30]R. Wu, B. Yang, J. Xiong, C. Cao, Y. Huang, F. Wu, J. Sun, C. Zhou, H. Huang, and J. Yang, J. Renewable Sustainable Energy **7**, 043105 (2015).
[31]B. Prasai, B. Cai, M. K. Underwood, J. P. Lewis, and D. A. Drabold, J. Mater. Sci. **47**, 7515–7521 (2012).
[32]See http://shop.solaronix.com/titania-pastes/ti-nanoxide-t-sp.html for "Solaronix" (last accessed May 7, 2018).
[33]See https://www.sigmaaldrich.com/catalog/product/aldrich/793833?lang=en&region=US for "Sigma-Aldrich" (last accessed May 10, 2018).
[34]See http://www.commonorganicchemistry.com/Common_Reagents/Dimethylformamide/Dimethylformamide.htm for "Dimethylformamide (DMF)" (last accessed April 2, 2019).
[35]B. Bhattarai, A. Pandey, and D. A. Drabold, Carbon **131**, 168–174 (2018).
[36]See https://www.mtixtl.com/LargeAutomaticFilmCoaterwith12Wx24LVacuumChuck-MSK-AFA-II-VC.aspx for "MTI" (last accessed April 2, 2019).
[37]J. Peng, L. Lu, and H. Yang, Renewable Sustainable Energy Rev **19**, 255–274 (2013).